Date: ____1/3/2020_____

EIC Detector R&D Progress Report

Project ID: eRD21__
Project Name: EIC Background Studies and the Impact on the IR and Detector
Period Reported: from_1 July 2019 to_31 Dec 2019
Project Leader: Latifa Elouadrhiri
Contact Person: _Latifa Elouadrhiri

Project members

1. Latifa Elouadrhiri: JLab physics
2. Charles Hyde: ODU physics
3. Vasiliy Morozov: JLab accelerator
4. Christine Ploen: ODU physics
5. Marcy Stutzman: JLab accelerator
6. Mike Sullivan: SLAC physics
7. Yulia Furletova: JLab physics
8. Mark Wiseman: JLab engineering
9. Andrey Kim: UConn physics
10. Vitaly Baturin: ODU physics
11. Youri Sharabian: JLab physics
12. Kyungseon Joo: UConn physics
13. Pavel Degtiarenko: JLab RadCon
14. Frank Marhauser: JLab RF
15. Alexander Kiselev, BNL Physics

Abstract

In this report we present this year progress on the studies of background effects related to the EIC interaction region and detectors using GEANT4 and FLUKA. In Section 1 we focus on the synchrotron radiation. We report on our recent progress on the simulation code for individual synchrotron photons emitted by electrons going through the JLEIC lattice described in the code in terms of standard linear beam optics. The developed code is used for the GEANT4 simulations described in Section 2. In Section 3 we report on a dedicated effort we put in place to the study of the neutron backgrounds in the Experimental Hall and present preliminary results. In Section 4 the issues related to the man power, funding, and publications are addressed.

Table of Contents

1. Simulation of Synchrotron Radiation in JLEIC lattice

1.1 Synchrotron Radiation Generation

We use a semi-analytic simulation program SYNC_BKG to efficiently simulate the synchrotron power generated by the electron beam in the final focus electron quads upstream of the interaction point (IP). SYNC_BKG was developed at SLAC for PEP-II, and is based on an earlier code SYRAD, written at LBL by A. Clark for PEP. Each quadrupole is divided into four ideal segments. As electrons propagate through a segment, the total synchrotron radiation power is calculated analytically for that segment, based on the local (approximated as constant) radius of curvature of the electron trajectory. The synchrotron power for each segment is distributed uniformly over the tangent directions of the electron. Although the advanced analytical SYNC_BKG program precisely calculates all SR effects it can not be used in the Geant4 environment since the latter requires individual SR photons for a further propagation along the beam line and detector components located downstream the interaction region.

1.2 Progress

The program SYNC_BKG was carefully studied and modified with the only goal to generate a file with SR photons in a form that comply with Geant4 requirements. The modified program SYNC_BKG is named as SYRAD.FOR. Being a further modification of SYNC_BKG, this program rasters a bunch of 0.93E+10 electrons over the XY plane at the lattice entry, with the electron beam entry coordinates are randomized accordingly to the specified electron beam profiles.

For each instant of the electron bunch entry to the lattice the total energy of SR ray is scaled by XY-dependent weight defined by electron beam profiles. Therefore the total amount of electrons passed through the lattice is equivalent to one bunch smeared over the lattice entry.

The beam profiles in transverse phase space include the coordinate and directional Gaussian distributions corresponding to the beam emittance, plus a fraction of the beam in a broader Gaussian tail — consistent with PEP-II experience. The beam tail produces significant SR power in the quadrupoles, since the electron trajectory curvature in quad magnets is higher at higher distances from the beam axis.

The photon emission z-coordinates, as well as x, y coordinates and corresponding directional angles are uniformly randomized by SYRAD.FOR between the far and near points of each segment of each quadrupole magnet as given by the original program SYNC_BKG.

The photon energy simulation was done in a different way. As a core of SYRAD.FOR the SYNC_BKG provides the total energy generated by the electron bunch in the magnet. This energy is considered by SYRAD.FOR as a “thermostat” from which it consumes the energy for each individual photon. A random photon energy is generated from the nominal SR distribution which is characterized by the critical energy attributed to the electron trajectory inside a certain quadrupole magnet. This randomized photon energy is subtracted from the thermostat and a new photon is similarly generated until all of the “thermostat” for that segment is exhausted. Each generated photon is recorded into the output file in LUND format for further Geant4 studies. The properties of the simulated photons are demonstrated in Figs.1-1,1-2, and 1-3.

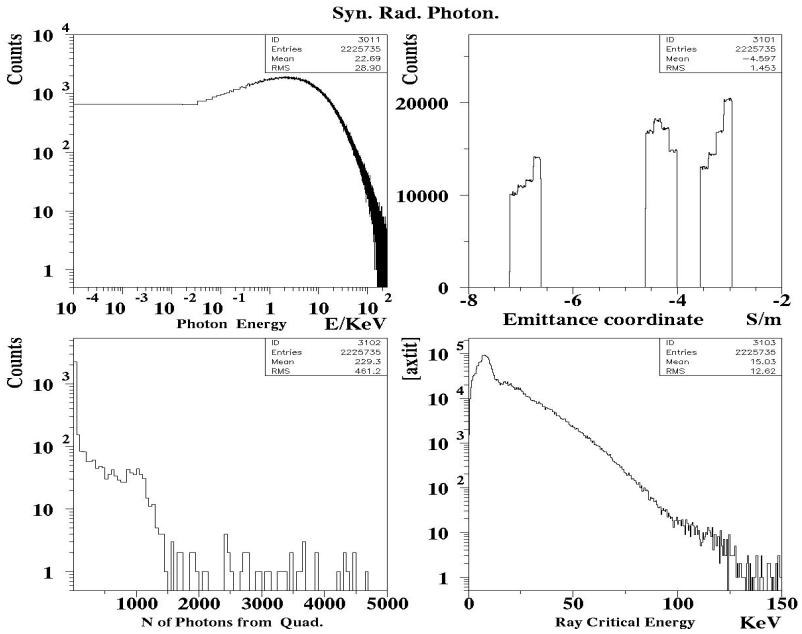

Fig.1-1. Characteristics of Simulated SR photons. Top-left: nominal SR-photon energy distribution. Top-right: Z-coordinate distribution of generated photons; three quadrupole magnets are seen at corresponding coordinates, each subdivided into four segments. Bottom-left: number of photons in SR ray. Bottom-right: SR ray critical energy distribution.

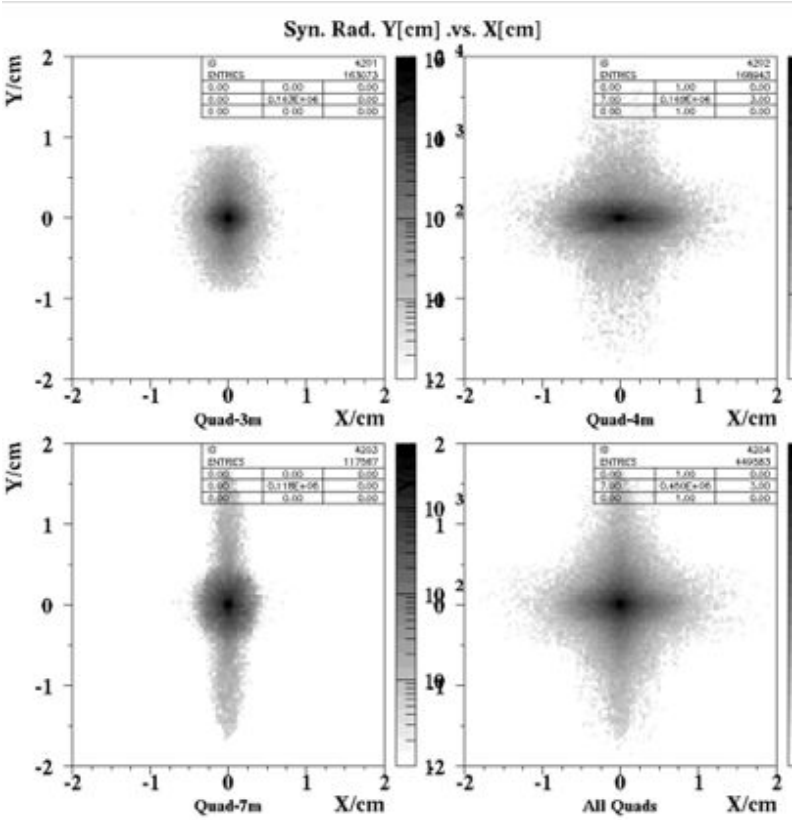

Fig.1-2. Photon flux emitted from three quadrupole magnets. **Top-left:** from the Quad at S=3 m. **Top-right:** - at S=4 m. **Bottom-left:** - at S=7 m. **Bottom right**: the flux from all three magnets.

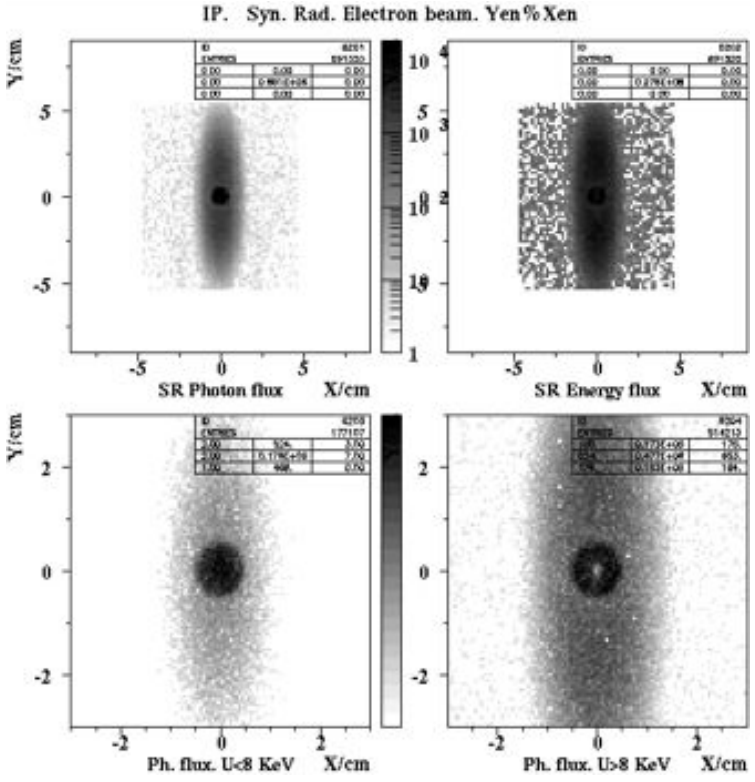

Fig.1-3. Profiles of parent electrons at the entry to the lattice. Profiles are given for various intervals of SR photon energy. **Top-left:** electron beam profile for all emitted SR photons. The central core and beam halo are visible. **Bottom-left:** same, but provided photon energy below $8\,KeV$; low energy photons are generated in the weaker field closer to the beam axis, as expected. **Bottom-right:** same for photon energy greater than $8\,KeV$; the expected enhancement of SR-photon flux at higher transverse distances is clearly seen. **Top-right:** SR energy weighted distribution of electrons at the lattice entry; the rectangular raster of parent electrons is clearly seen in this plot.

1.3 Future plan

The SYNC_BKG and SYRAD.FOR are installed and operational at Jefferson Lab. The documentation including tutorial will be made available in the next phase of this project. The plots shown above are in agreement with natural expectations of Synchrotron Radiation. The next section shows our results for the GEANT4 simulation of these synchrotron photons as they traverse the Interaction Region (IR). Photon parameters are recorded in LUND format and each photon record contains the integrated beam current up to the moment of a photon emission. The generated SR photons may be used by Geant4. Photon files are placed to JLAB storage in order to be used for Geant4 simulation of the interaction region.

Future work can add additional beam line elements (anti-solenoid, crab cavities…). Near term, we are ready to apply this code to the eRHIC electron beam and IR transport. Meeting with eRHIC group will be scheduled early this year.

2: GEANT4 Simulation of Synchrotron Radiation in the Interaction Region

We have taken the LUND files of synchrotron photons, as described in the previous section, and propagated them through a GEANT4 simulation of the Interaction Region (IR), as illustrated in Fig. 2-1. The model includes two beam pipes crossing at 50 mrad, with a central 3cm radius water cooled Be chamber 20 cm long. The Be chamber also has a thin plating of Au, to absorb synchrotron photons. Fig. 2-2 shows a close-up, with the layers of the Silicon Vertex Tracker (SVT) clearly visible.

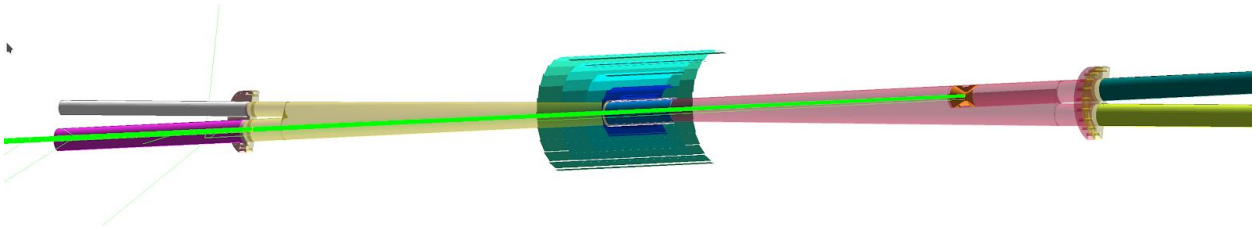

Fig 2-1. Top view of GEANT4 model of beam pipe and SVT. Synchrotron photons (in green) are shown as they emerge from the 1.2 cm radius Cu collimator 1 m upstream of the IP.

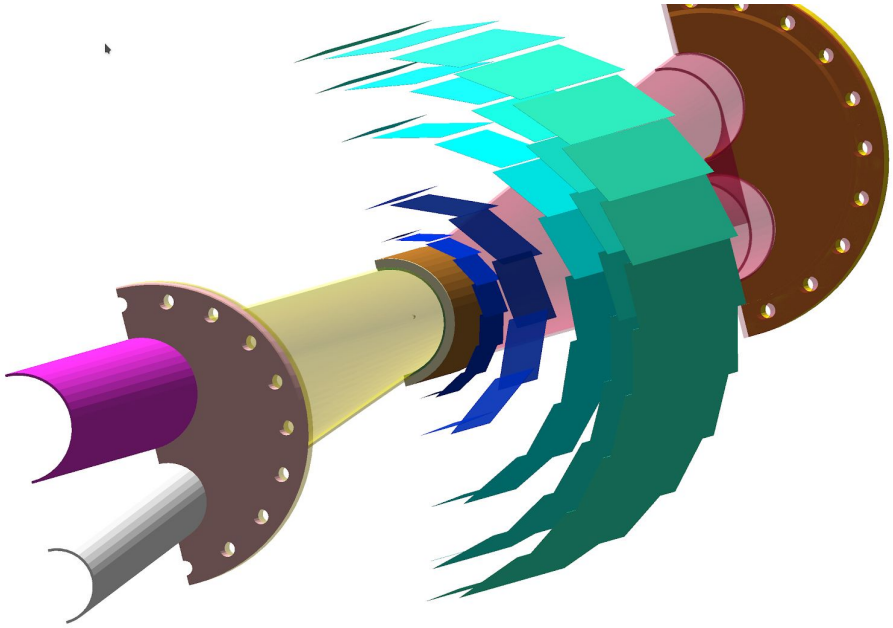

Fig. 2-2. GEANT4 model: Zoom of top view, looking in direction of propagation of the ion beam, entering at lower left. The five layers of the Silicon Vertex Tracker are clearly visible.

2.1 Synchrotron Deposition Results

In Fig 2-3, we show all synchrotron photon hits in the SVT and the central 20 cm long Be beam pipe. These synchrotron photons are generated by $1.02 \cdot 10^{11}$ electrons at 10 GeV. The nominal JLEIC electron beam current at 10 GeV is 0.8 Amp, or $5 \cdot 10^{18}$ electrons per second.

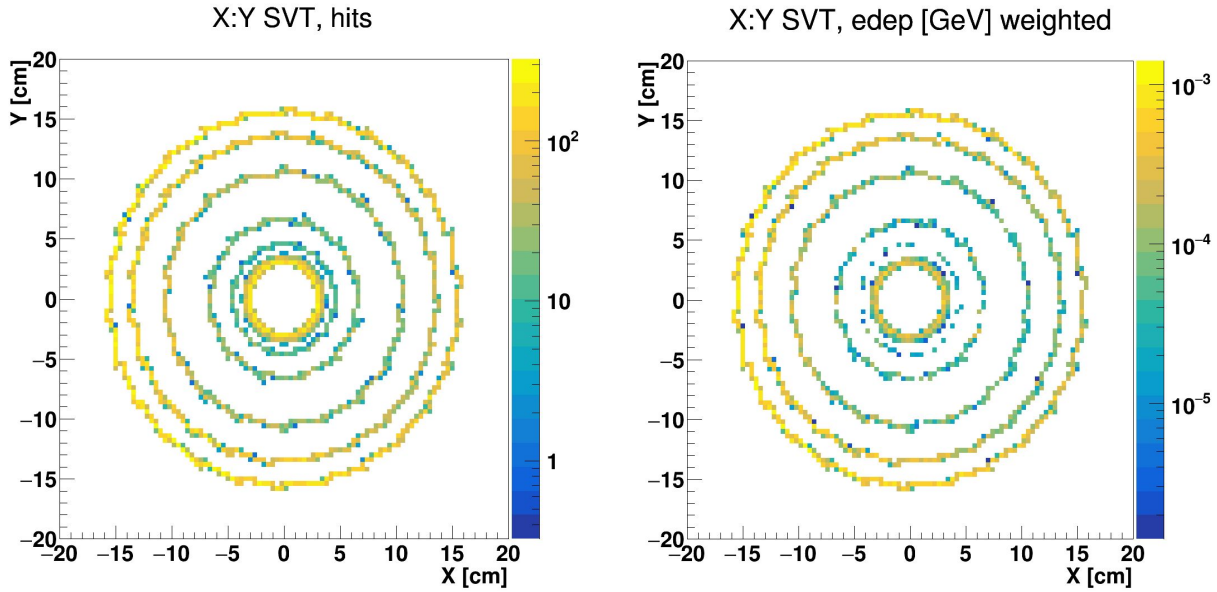

Fig. 2-3 Synchrotron radiation hits in the central beam chamber (Be plus water cooling channel) and five Silicon Vertex Tracker (SVT) layers. Hits are integrated over the full length of each SVT layer and the 20 cm long central chamber. Left: Raw hits per $1.02 \cdot 10^{11}$ incident electrons. Right: Hits weighted by deposited synchrotron energy (GeV).

Fig 2-4 displays the total energy deposition from this synchrotron bunch in each of the five layers of the SVT, with layer 0 corresponding to the Be chamber. The total power, in GeV/sec is obtained by scaling these results by $(5 \cdot 10^{18} e^{-}/\text{sec})/(1.02 \cdot 10^{11}\ e^{-}) = 4.9 \cdot 10^{7}$/sec. For example the power in the Be pipe is (22 MeV)$(4.9 \cdot 10^{7}$/sec) = $6.5 \cdot 10^{8}$MeV/sec, or 0.17 milliWatt. On the other hand, the total energy in the synchrotron bunch continuing to the 0° Bremsstrahlung line is 51.5 TeV, for a power deposition of 400 Watt. The dose rates in each layer of the SVT are calculated in Table 2-1. These dose values are independent of the Si pixel/strip sizes and readout times, and are roughly independent of sensor thickness and support structure.

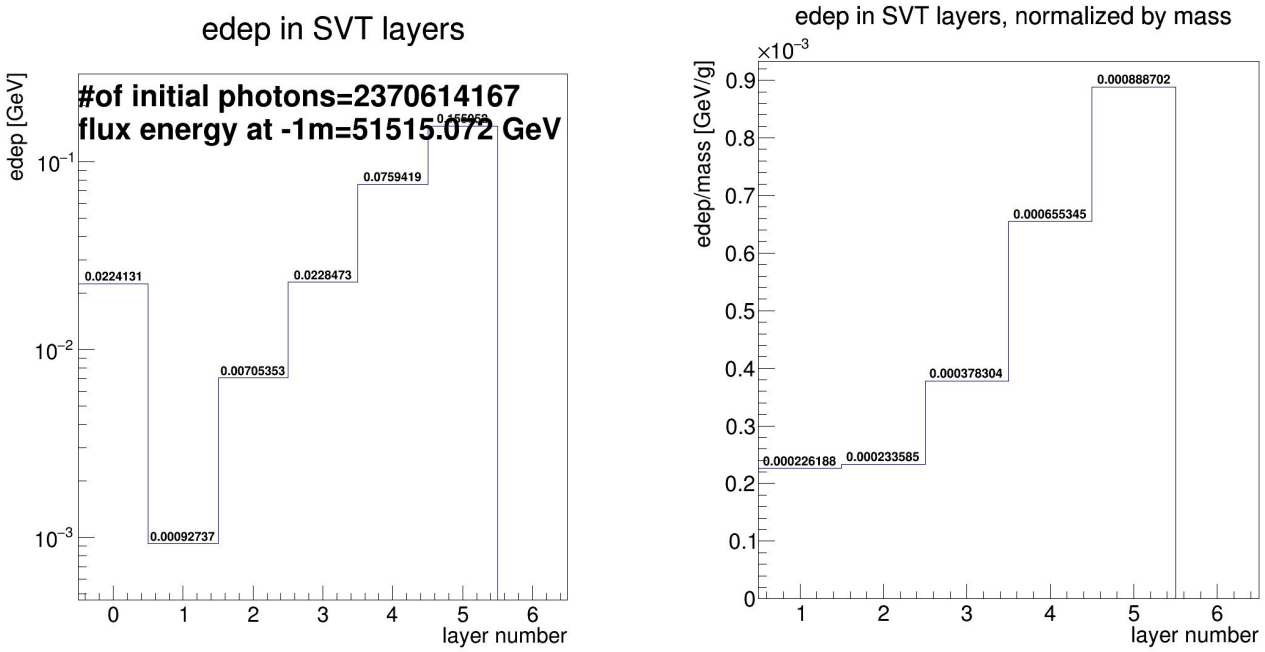

Fig.2-4: Left Plot: Integrated synchrotron energy deposition in each layer of the SVT, per $1.02 \bullet 10^{11}$ beam electrons. Layer 0 is the Be beam pipe. **Right Plot:** Energy deposition dose, in units of GeV/gram in each SVT layer. Scaling by $4.9 \bullet 10^{7}$/sec equivalent electron bunches (0.8 A) yields the total power deposited in each layer (left) and the dose rates (right)

Table 2-1: Synchrotron Energy Deposition per $1.02 \bullet 10^{11}$ e^{-}@10GeV in each SVT layer. Mass of each layer, and Synchrotron radiation dose rate in each layer. One year is assumed as 10^{7} sec.

SVT Layer	1	2	3	4	5
Energy Deposition	$9.3 \bullet 10^{-4}$ GeV	$7.1 \bullet 10^{-3}$ GeV	$2.3 \bullet 10^{-2}$ GeV	$7.6 \bullet 10^{-2}$ GeV	$1.6 \bullet 10^{-1}$ GeV
Mass	4.1 g	30.2 g	60.4 g	115.9 g	174.5 g
Dose rate (GeV/g/sec)	$1.1 \bullet 10^{4}$	$1.2 \bullet 10^{4}$	$1.9 \bullet 10^{3}$	$3.2 \bullet 10^{4}$	$4.5 \bullet 10^{4}$
Dose rate (KGray/year)	17.7	18.4	29.8	51.3	71.7

2.3 Future Work

In future work, we will incorporate alternate SVT models, including support structures, as available. We will also initiate a synchrotron radiation simulation of the eRHIC IR.

We will work closely with the EIC users group leadership to determine the immediate need from our background simulation group to guide the detector design and readout electronic choices.

3. Simulation of Neutron Background in the JLEIC Experimental Hall

3.1 Introduction Research Plan

A dedicated effort was put in place to study the neutron background rate as recommended by the review committee. The team consists of physicists, accelerator physicists and radiation physicists. The study includes simulations using different simulation tools as well as the planning of experiment to measure the neutron rate that will take place at Jefferson Lab in Hall B in early 2020. In this section we will present out preliminary results using FLUKA.

The main goal of the neutron flux studies with FLUKA is to estimate the low energy neutron fluence through the Si-based detectors in the environment of the experimental hall and to find a remedy to bring the fluence to acceptable levels, if necessary. Therefore, prior to creating a very complex fully realistic model, it is useful to study the properties of the thermal neutron fluxes — their dependence on the experimental hall environments — using simplified models which include the main sources of thermal and epi-thermal neutrons. The sources considered here include residual gas in the ion beam pipe, the beam pipe itself, lattice magnet materials, the

main detector elements, and the experimental hall walls and floor. Below we report on our initial studies of the neutron fluence generated by 100 GeV/c proton beam propagating through the ~70 m long upstream ion beam line from the last bend in the arc.

3.2 Progress.

The corresponding FLUKA model is shown in Fig.3-1 together with JLEIC Hall design. The Detector design is close to that from the GEANT4 model shown in Fig.3-2 in comparison with FLUKA model.

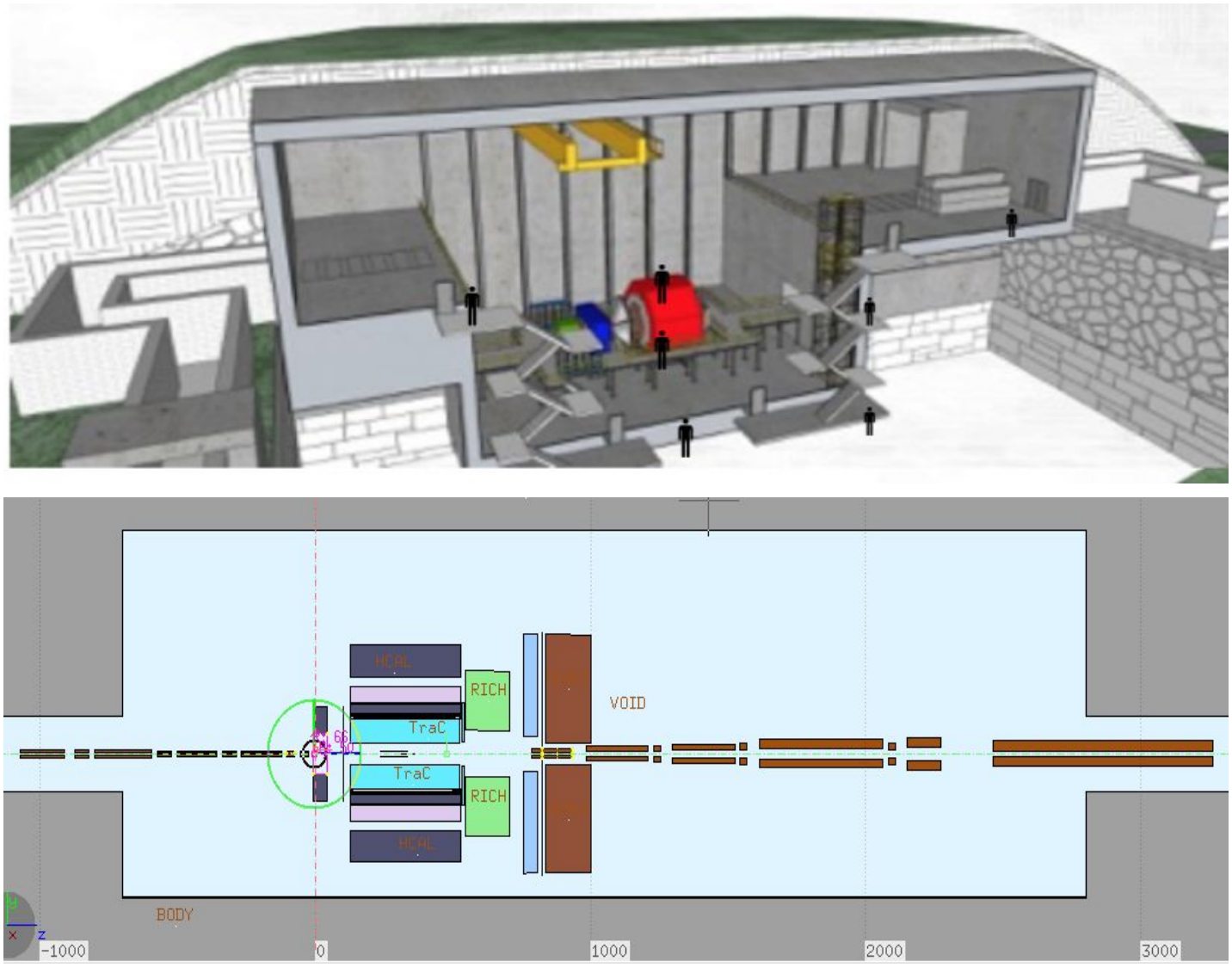

Fig.3-1 Top image: JLEIC engineering design of Experimental Hall. Bottom image: Simplified model of JLEIC Experimental Hall, ion beamline and Detector for FLUKA simulations. The Hall is roughly 35 m long. Horizontal scale is given in cm.

.

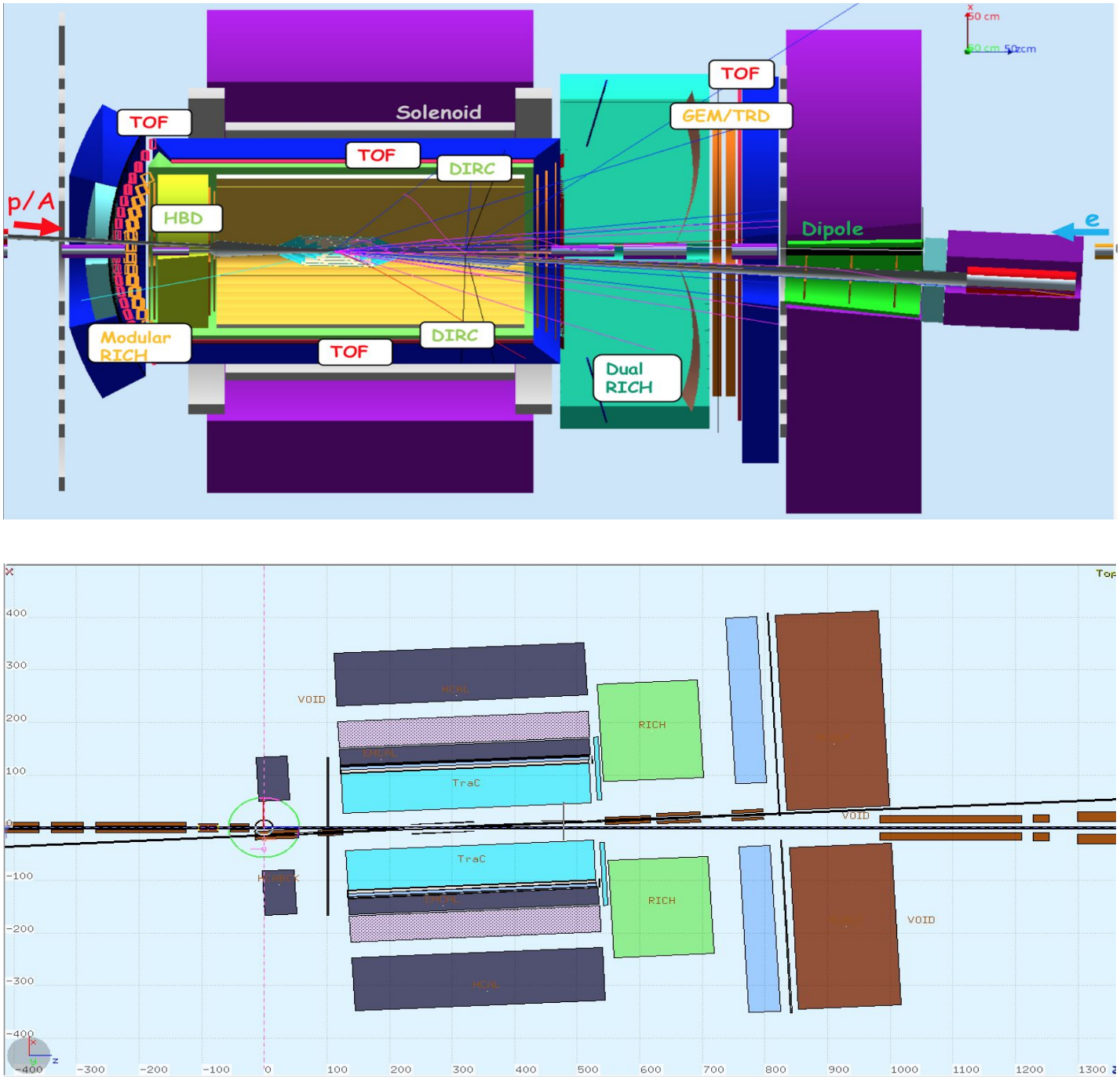

FIg. 3-2. The JLEIC detector from GEANT4 model (top picture) in comparison with FLUKA model (bottom picture). The FLUKA image is rotated 50 mrad compared to the GEANT4 image, placing the ion beam in the horizontal direction of the FLUKA image.

The FLUKA model contains the following objects:

1. Metro Station like Hall made of Concrete with 2 tunnels for electron and ion beams.
2. Central aluminum X-pipe with the center in the Interaction Point.
3. Central cylindrical pipe around IP made of Beryllium.
4. Ion and electron beam quadrupole magnets with their volume filled with a mixture of Iron, Copper, and water.
5. Central detector Solenoid made of a mixture of Tin, Copper, and Helium.
6. Calorimeters (Barrel, Forward, and Backward) filled with Lead and Scintillator mixture.
7. Trackers - central and forward -filled with Argon.
8. Silicon based detectors -SVT and SiPMs.
9. Air in the experimental Hall.
10. Vacuum in the beam pipes with a central (1mm-diameter) “pencil” of Air at 100 mbar along the exact beam line.

The primary particle history is a sequence of interactions of secondary particles resulting from the probable interactions of beam particles with the residual gas. In this FLUKA model, the residual gas forms a very narrow (1 mm in diameter) cylinder inside the beam pipe. Low pressure and low diameter of this air cylinder allows to neglect interactions of secondary particles with residual gas inside the beam pipe. This approximation speeds computation time, while still allowing linear rescaling of the results to realistic values of the very low gas pressure in the vacuum beam pipe.

All FLUKA calculations presented in this report: Neutron fluence, dose, and energy deposition, are per incident proton at the artificial beam-gas pressure of 0.1 Bar along the beam-axis. In order to estimate the counting rate one has to scale the resulting fluence by the air pressure factor for $P=10^{-9}$ mbar of the nominal vacuum pressure and

by the ion beam intensity (0.75 A) in particles per second. The same factors apply to the results for dose and the energy deposition.

The following values are addressed by FLUKA are presented in the figures:

1. Energy deposition is given in GeV/cm^3 per primary particle history.
2. Dose is given in GeV/g per primary particle history. Dose in units of Gy is the Dose in GeV/g multiplied by 1.602E-7.
3. Fluence is given in particles/cm^2 per primary particle history.

In order to estimate rates for energy deposition, dose, and fluence, the numbers in the following figures should be multiplied by the beam intensity of $4.7 \cdot 10^{18}$ protons/sec (nominal beam current 0.75 A) and beam vacuum ratio P/P_0 = (10^{-12} bar)/(0.1 bar) = 10^{-11} for a net scaling factor of $4.7 \cdot 10^7$/s to obtain rates per sec. Similarly, to obtain the neutron dose in one year of running, multiply by an additional factor of 10^7 sec. The standard "year" of 10^7 sec yields an integrated luminosity of 100/fb at instantaneous luminosity of 10^{34}/cm^2/sec.

Examples of the energy deposition map, neutron fluence map and the dose map are shown in Fig.3-4. The neutron fluence map illustrates that the detector itself, the experimental hall walls, and beam line elements act as neutron sources. The neutron dose to the photo-sensors of the electron-side modular RICH detector is roughly 10^{-8} GeV/g per incident proton, with a maximum of 10^{-7} GeV/g per incident proton. Note that these doses are roughly independent of the technology (MCP, SiPMT) or thickness of the sensors. The DIRC photo-sensors would receive a similar dose of 10^{-8} GeV/g per incident proton. Normalizing by a 0.75 A proton current for 10^7 sec, and the assumed beam vacuum of 10^{-9} mbar, the DIRC sensors and outer mRICH sensors would receive doses of 0.75 Gy per year of operations. The innermost mRICH sensors would receive a dose 10x greater. In contrast, the photo-sensors of the ion-side dual RICH (which are located in the shadow of the solenoid coil) would receive an estimated annual dose of 0.075 Gy.

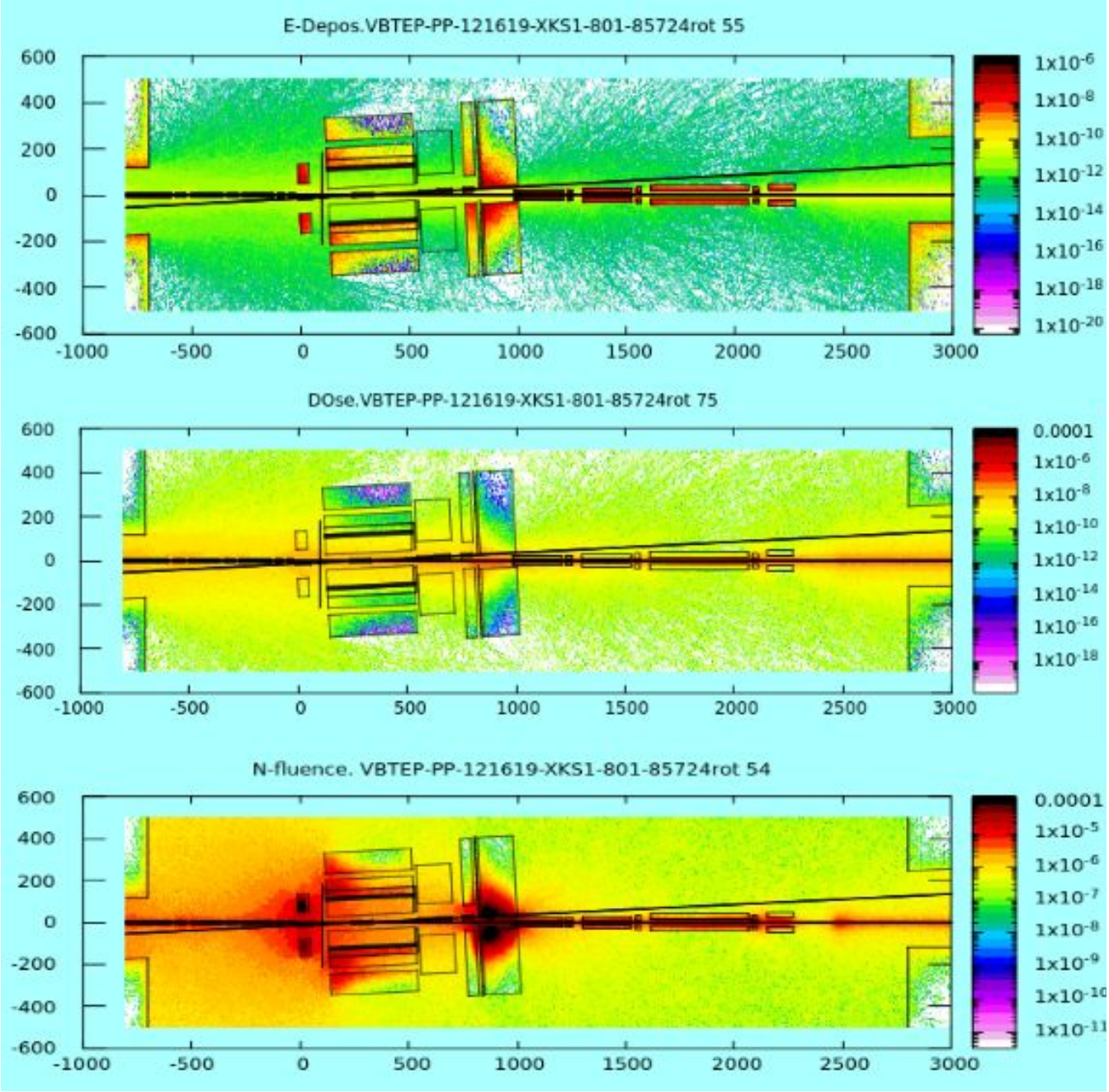

Fig. 3-4 Fluka maps. Vertical scale-Y-coordinate in cm. Horizontal scale-Z in cm.**Top:** Energy deposition in GeV per cm^3 per beam particle history (colour chart at the right side of the scatter plot). **Middle:** Dose in GeV per gram per beam particle history. **Bottom:** Neutron fluence given in units of particles per ($cm^2 \cdot sr$) per beam particle history. Multiply all values by $4.7 \cdot 10^6$/s to obtain appropriate rates per sec. Multiply all values by $4.7 \cdot 10^{13}$ to obtain yearly totals.

Typical energy spectra of neutron fluence are shown in Fig.3-5. Neutron fluence is the gross inward fluence for the entire surface of three sample volumes and is given in units of particles per GeV per primary history. Fluence must be normalized by the beam intensity in primaries/s, and air pressure factor (P/P_0).

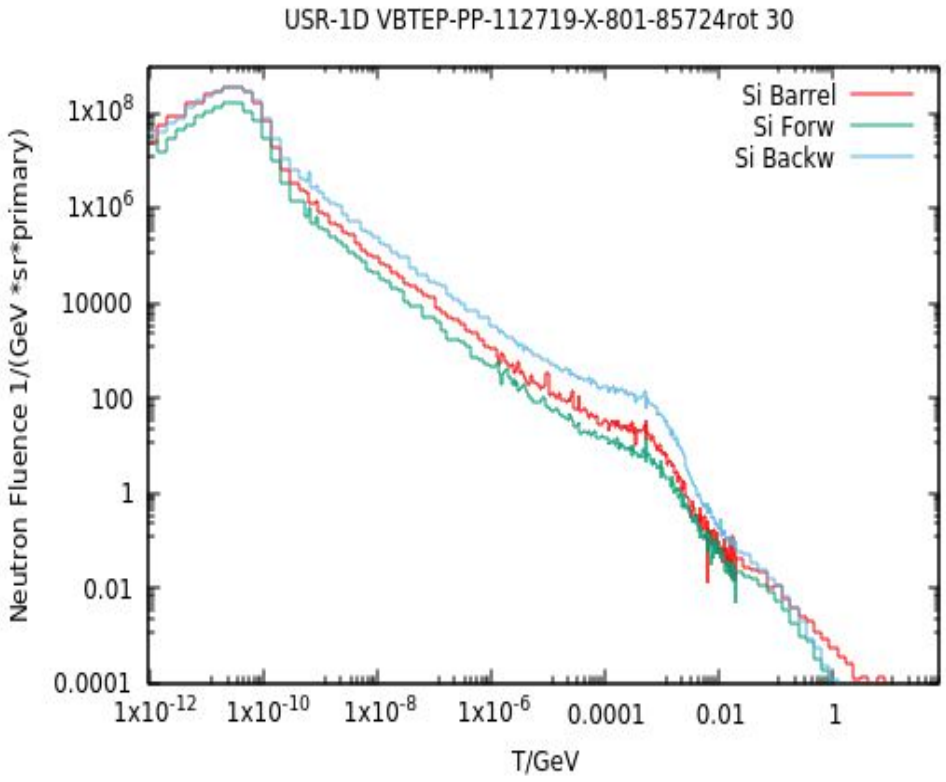

Fig.3-5. Differential neutron fluence vs. neutron energy. Neutron fluence is given for the entire surface of three sample cylindrical annuli of length *L* and radii r_1, r_2. For SVT (red): *L=100cm, (r_1, r_2) = (8.5,9.0) cm, and Area = 11,060 cm^2.* For both Backward Si (ion-upstream=blue) and Forward Si (ion-downstream = green): *L=1.0cm, (r_1, r_2) = (110,125) cm, and Area = 23,600 cm^2.*

From Fig.3-5 we observe that contrary to expectations, the n-fluence in the upstream area (photo-sensors for either modular RICH or DIRC) shown as blue histogram is about 20 times higher than the fluence in the downstream area (photo-sensors for dual RICH) plotted as green histogram. The reason for that is clear from the n-fluence map shown in Fig. 3-4. According to this map the upstream calorimeter, as well as the beam

line magnets act as neutron sources. Another illustration of this fact is given in Fig.3-6 that compares neutron fluence maps with and without the upstream calorimeter.

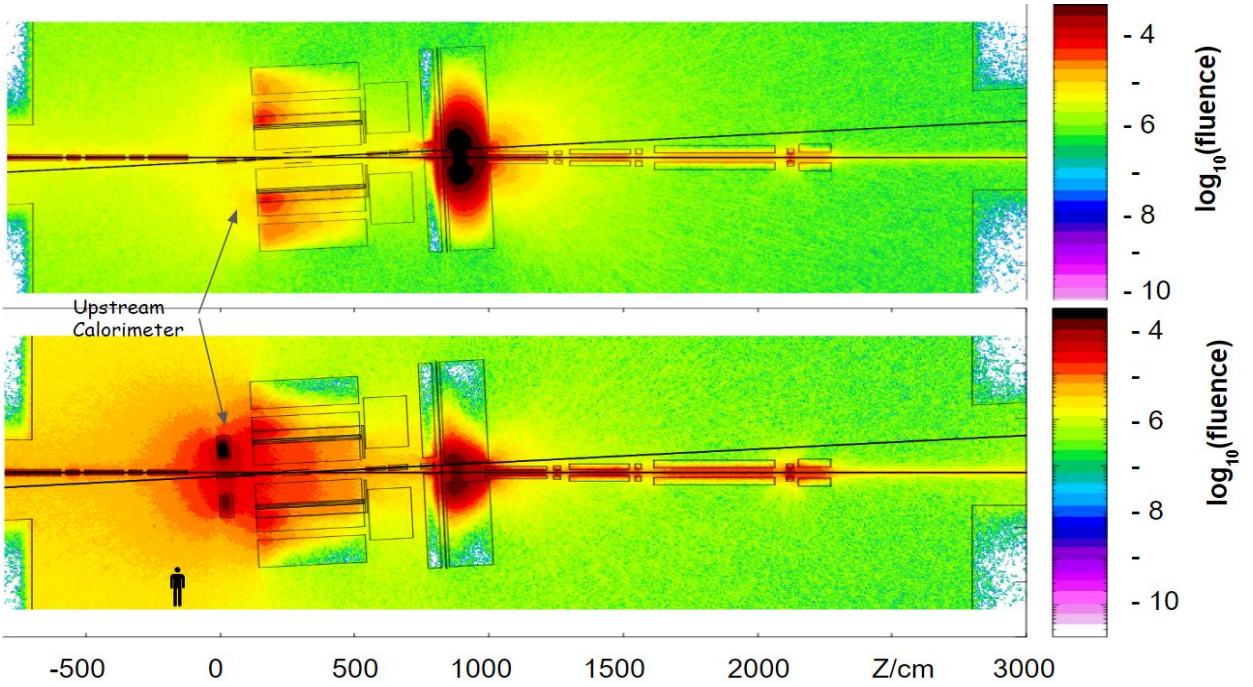

Fig.3-6 Neutron fluence maps. Effect of the Upstream (Backward) EM calorimeter. Vertical scale -Y coordinate in cm. Horizontal scale - Z-coordinate in cm. **Top:** neutron fluence map without the upstream EM calorimeter. **Bottom:** neutron fluence map with the Upstream (electron downstream) EM calorimeter. The calorimeter increases the neutron fluence on the ion-upstream half of the central detector, while reducing the fluence on the ion-downstream end-cap detectors.

Figs. 3-7 and 3-8 show zooms of the central detector surrounding the Interaction Point (IP). In Fig. 3-7, in particular, we see that the dose (all particles) in the Si Vertex Tracker is approximately 8 Gy per year of operation. This is largely independent of the actual construction details of the SVT. In future work, the simulation will be updated to a more realistic model of the SVT, with layers closer to the beam pipe, which will receive higher doses.

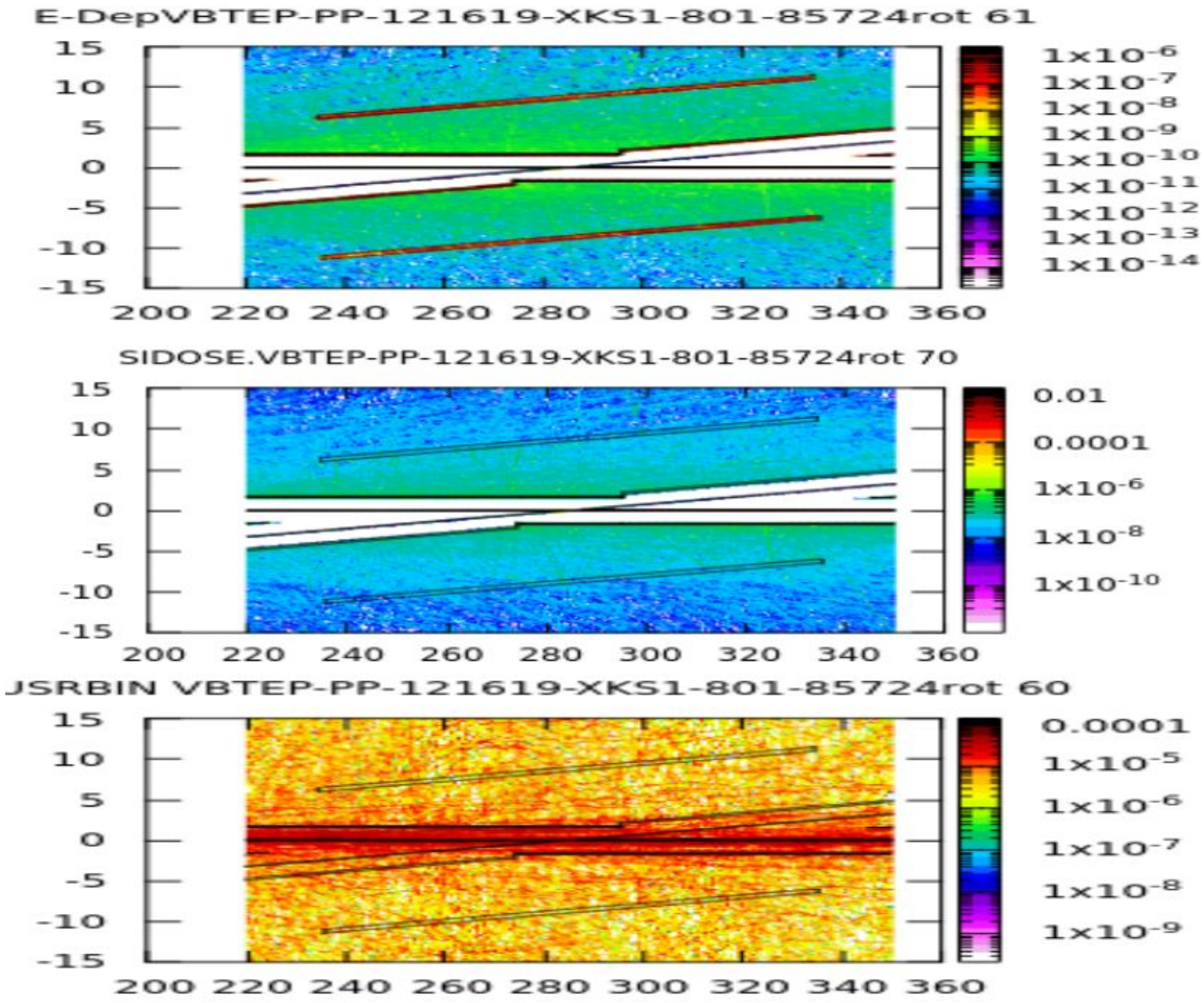

Fig.3-7. FLUKA model of the Interaction regions inside JLEIC detector; 1cm thick X-slice. Vertical scale-Y-coordinate in cm. Horizontal scale-Z in cm. **Top:** Crossing beam-pipes and the Si Vertex Tracker (SVT) are both seen in the Energy Deposition Map. **Middle:** Dose Map. **Bottom:** Neutron Fluence Map. A very narrow "pencil" of residual air at 0.1 bar is clearly seen on these maps. The dose in the SVT in one year of full exposure is approximately $(10^{-7}\text{GeV/g})(4.7\bullet10^{14}) \sim 5\bullet10^{7}\text{GeV/g}$ or 8 Gy per year of operations.

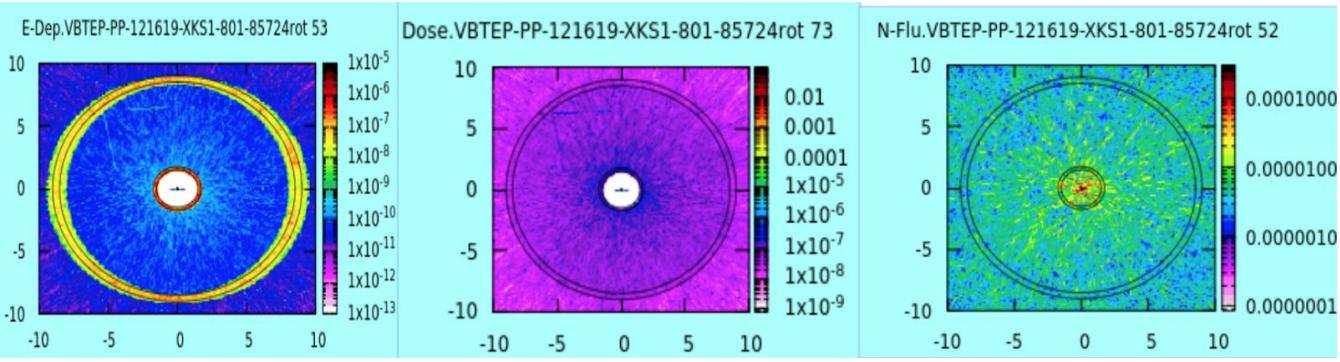

Fig.3-8 FLUKA maps across the detector. Z-slice 20 cm thick, centered at collision point. Vertical scale: Y-coordinate in cm. Horizontal scale: X-coordinate in cm. **Left:** Energy deposition map. **Middle:** Dose map. **Right:** Neutron fluence map. The annulus between radii of 8.5 and 9.0 cm represents the initial SVT model.

3.3 Summary and Future plan

Summary:

- A realistic FLUKA model of the JLEIC Experimental Hall and the Detector is constructed.
- Preliminary estimations of the neutron fluence through the Silicon based detectors are performed for the proton beam.
- It is shown that the experimental hall walls and floor, the detector itself, and beam line elements act as neutron sources.
- From the neutron fluence map we conclude that the fluence through detectors at the downstream side of the detector barrel is several times lower than comparable positions at the upstream side.

For the next six months we plan to:

- Improve the model with more detailed detectors and beam line elements.
- Perform n-fluence calculations with electron beam
- Develop simulation of eRHIC and RHIC configurations, and compare to existing eRHIC simulations and RHIC data.
- Evaluate potentiality of alternate simulation codes, e.g. MARS
- Participate to the Hall B experiment scheduled in early 2020 to measure the

neutron rate and compare the results with different simulation tools.

4.Manpower, Funding, Publications

- 4.1 Manpower
  - **Vitaly Baturin:** (post-doc) JLab/ODU, ODU supervisor Charles Hyde, JLab Supervisor Latifa Elouadrhiri. 100% on project. Supported 50% FTE from project funds, 35% FTE from CFNS-SBU, and 15% from ODU DOE research grant. Anticipated travel to BNL/SBU in early 2020.
  - **Christine Ploen:** JLab/ODU, ODU supervisor Charles Hyde, Lab Supervisor Latifa Elouadrhiri. Supported 100% on ODU Graduate Teaching Assistantship (GTA) during reporting period; supported effort on project was 10%FTE. During January-May 2020 Christine will be supported 100% on eRD21 FY2020 project funds, with full research effort on project (50% FTE, as mandated by federal law).
  - **Andrey Kim:** (post-doc) UConn/JLab, UConn supervisor Kyungseon Joo, JLab Supervisor Latifa Elouadrhiri. Support 50% FTE from eRD21
  - **Other Personal:** listed on the cover page. No direct support from project. Effort various, consistent with the progress of supported personnel.

4.2 External Funding

Specific funding for students, post-docs is described in section 4.1. Travel support for C. Hyde provided by D.O.E. research grant.

4.3 Publications and talks

EIC machine backgrounds" at the workshop on "Forward Physics And Instrumentation From Colliders To Cosmic Rays" held at the Center for Frontiers In Nuclear Science (CFNS) at Stony Brook University, New York between October 17th and 19th, 2018:

"Background in EIC and HERA Lessons" C. Hyde, L. Elouadrhiri, Plenary invited talk at EIC Users Group Annual meeting, Paris, France, 22–26 July 2019.

Beam Gas Studies at HERA publication in preparation.

5.Previous Results of Beam Gas Studies

For completeness, we present in Fig.5-1 our previous beam gas background study, which reproduced the HERA-II measurements within a factor of two.

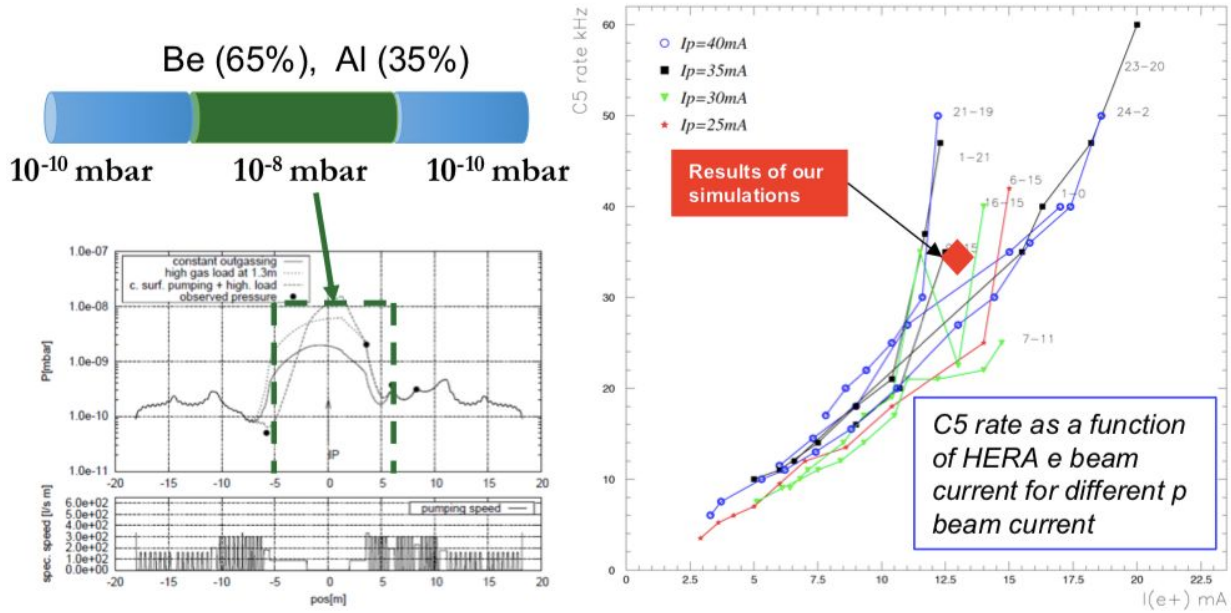

Fig.5-1. Background results from HERA-II. **Left plot:** Inferred beam vacuum profile. Dotted green line is the model we used in GEANT4 study. **Right Plot:** HERA-II background measurements vs. beam current (small dots with lines). Large red diamond is the result of our GEANT4 study.